Influence of the cathode catalyst layer thickness on the behaviour of an air breathing PEM fuel cell

Paloma Ferreira-Aparicio and Antonio M. Chaparro[*]

Department of Energy, CIEMAT, Avda. Complutense 40, 28040 Madrid, Spain

Abstract. Fuel cells of proton exchange membrane type (PEMFC) working with hydrogen in the anode and ambient air in the cathode ('air breathing') have been prepared and characterized. The cells have been studied with variable thickness of the cathode catalyst layer (L_{CL}), maintaining constant the platinum and ionomer loads. Polarization curves and electrochemical active area measurements have been carried out. The polarization curves are analyzed in terms of a model for a flooded passive air breathing cathode. The analysis shows that L_{CL} affects to electrochemical kinetics and mass transport processes inside the electrode, as reflected by two parameters of the polarization curves: the Tafel slope and the internal resistance. The observed decrease in Tafel slope with decreasing L_{CL} shows improvements in the oxygen reduction kinetics which we attribute to changes in the catalyst layer structure. A decrease in the internal resistance with L_{CL} is attributed to lower protonic resistance of thinner catalyst layers, although the observed decrease is lower than expected probably because the electronic conduction starts to be hindered by more hydrophilic character and thicker ionomer film.

Keywords: fuel cell; PEMFC; hydrogen; oxygen reduction; portable application

1. Introduction

Fuel cells are becoming increasingly interesting for portable devices with medium-low power requirements due to their possibilities to improve power density and autonomy. Among different types, low temperature fuel cells with proton exchange membrane electrolyte (PEMFC) are closer to the massive application. Weight and space limitations requirements on portable applications make necessary the use of 'air breathing' cathodes, i.e., cathodes able to react with unforced ambient oxygen, in so called air-breathing PEMFC (AB-PEMFC) (Heinzel *et al.* 2002, Meyers *et al.* 2002, Chang *et al.* 2002, Giddey *et al.* 2010, Weiland *et al.* 2013, Fernández-Moreno *et al.* 2013). This cathode type allows for important system simplifications, however they have demanding working conditions since the passive reaction with ambient oxygen poses some limitations. Ambient oxygen flowing naturally through a standard gas diffusion electrode limits maximum attainable current densities to values below 1 A·cm^{-2}, which supposes maximum power generation rates in the range of 0.5 W·cm^{-2}. This value is still within applicability for many portable applications (medical, electronics, toys). Probably the most limiting factor becomes water

---

[*]Corresponding author, Researcher, E-mail: Antonio.mchaparro@ciemat.es

generated within the cathode catalyst layer (CL) from oxygen reduction ($O_2 + 4H^+ + 4e^- \rightarrow 2H_2O$), which must flow by unforced capillary transport and diffusion. Such transport mechanism is not fast enough, so water accumulation occurs within the cathode and also the anode (after diffusion through membrane), limiting power generation density below the mentioned limit. In order to be able to optimize cathode architecture, the careful characterization of electrode behavior is mandatory, with special attention to water transport parameters.

This work shows a study of the influence of cathodic catalyst layer thickness (L_{CL}) on the performance of single AB-PEMFC. The thickness of the catalyst layer is a critical parameter that influences mass transport and kinetics of oxygen reduction. Single AB-PEMFCs have been mounted with cathodic catalyst layers differing in the thickness, maintaining the same platinum load. The analysis of the polarization curves is carried out based on a standard model for a flooded catalyst layer (Cutlip 1975, Vogel *et al.* 1972, Stonehart *et al.* 1976, Lin *et al.* 2008). The information obtained on the influence of the CL thickness on cell performance is explained on the basis of this model by changes in the oxygen reduction catalysis and mass transport effects.

2. Experimental

Membrane electrode assemblies (MEA) have been prepared by electrospray deposition of Pt/C+ionomer (Nafion) on membrane as described elsewhere (Chaparro *et al*. 2011). For preparing cathode catalyst layer with variable thickness maintaining constant the catalyst load (0.17 $mg_{Pt} \cdot cm^{-2}$), three commercial Pt/C catalyst were used with variable Pt weight percent, namely 20 (ETEK), 40 (Alfa Aesar GmbH) and 60% (Alfa Aesar GmbH). The ionomer content was also maintained constant, at 15% weight percent, for the three catalyst layers. The membrane used was Nafion NRE212 with 13.7cm^2 active area. In cathode side, the electrosprayed catalyst layer is followed by a commercial gas diffusion layer (ELAT GDL LT1200W) and a gold plated Ni grid current collector (National Standard, 40×40 wires per inch, 0.005" wire diameter); finally the current collector is in contact (electrically isolated) with an end-plate made of stainless steel with an 8x8 matrix of circular openings (3mm diameter, 43 % aperture). For the anode, a commercial electrode has been used (ELAT GDE LT250EWALTSI, BASF, 0.25$mgPt \cdot cm^{-2}$), together with standard double serpentine channels flow field plate made of gold plated stainless steel (Grade 310S, 2mm thickness), a gold plated copper plate as current collector, and stainless steel end plate electrically isolated from the current collector. The two end plates clamp the MEA and other components by means of eight screws tighten to a controlled torque (4Nm). Photographs of the components and the air breathing single cell are shown in Fig. 1, and cross sectional scheme is in Fig. 2(a). The fuel cell works under constant anodic hydrogen flow (20 $scm^3 \cdot min^{-1}$); cathode is fed from quiescent ambient air, at room temperature and humidity (24 ℃ and 35%±5% RH). For AB-PEMFC characterization, polarization curves were measured in constant current step mode within a home made test bench station that allows for simultaneous measurement of the cell voltage and the internal resistance at 1kHz (Agilent Milliohmeter 4338B).

3. Model description

A flooded catalyst layer describes better the behaviour of the AB-PEMFC cathode due to the slow transport of water set by passive air breathing conditions. Water generated in the cathode
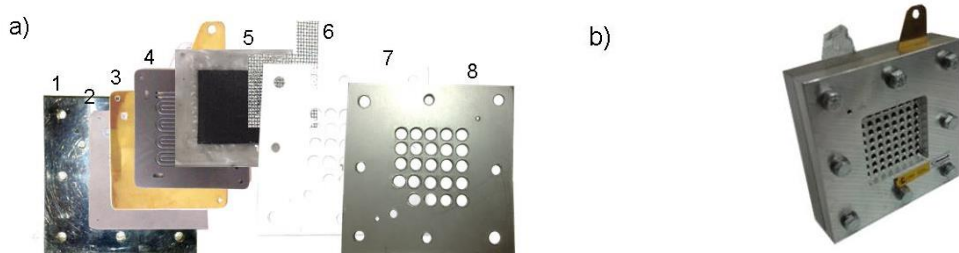
Fig. 1 (a) Scheme of the AB-PEMFC components: 1. Anodic end plate; 2. Gasket; 3. Anodic current collector; 4. Anodic flow field plate; 5. MEA; 6. Cathodic grid current collector; 7. Isolating layer; 8. Cathodic end plate, (b) Photograph of the assembled AB-PEMFC
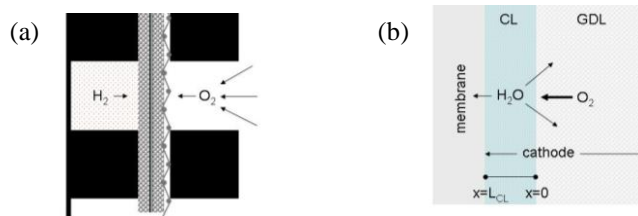

Fig. 2 (a) Cross sectional scheme of the AB-PEMFC, (b) Detail of the cathode side

catalyst layer flows in two opposite directions: diffusion through the membrane towards the anode, and evaporation through the gas diffusion layer (GDL). Both are particularly slow processes under passive air breathing conditions, which make the flooded catalyst layer a reasonable assumption. Taking this fact into account, the analysis of polarization curves has been carried out based on one dimensional model for a flooded agglomerate porous catalyst layer which considers both charge transfer kinetics and oxygen diffusion losses within the flooded pores (Cutlip 1975, Vogel *et al.* 1972, Stonehart *et al.* 1976, Lin *et al.* 2008). Such model allows for determining kinetics parameters and comparing the losses among different polarization curves, although not for information on mechanistic behavior. The model was initially developed for Teflon bonded gas diffusion electrodes, and provides an analytical solution that can be used for description fuel cell electrodes in phosphoric acid (Vogel *et al.* 1972, Stonehart *et al.* 1976) and proton exchange membrane (Lin *et al.* 2008) fuel cells. It assumes uniform overpotential distribution over the electrode thickness, which is appropriate for fuel cell gas diffusion electrodes as discussed in (Stonehart *et al.* 1976), and kinetics governed by first order oxygen reduction with Tafel behaviour, usually encountered in most oxygen reduction studies (Hoare 1967, Kinoshita 1992, Parthasarathy *et al.* 1992).

The model and basic assumptions are described below. Oxygen from ambient air dissolves in water which fills the pores of the gas diffusion layer (GDL) and diffuses towards the catalyst layer (CL) (Fig. 2(b)). The dissolved oxygen concentration at the GDL/air interface (c^*) depends on

oxygen partial pressure (p_{O2}) through Henry isotherm (Parthasarathy *et al*. 1992)

$$c^* = k_H \, p_{O2} \tag{1}$$

Where k_H (=$3.8 \cdot 10^{-6}$ mol·cm^{-3}·atm^{-1}) is the Henry isotherm constant of oxygen in water.

From the CL/GDL interface, dissolved oxygen diffuses inwards the reaction centers where it reduces, which is a process that can be described in the steady state by the transport equation

$$D_{CL} \, \mathrm{d}^2 c / \mathrm{dx}^2 = i/nF \tag{2}$$

Where c is the local oxygen concentration, i the local current density (both c and i vary with x dimension within the CL), D_{CL} is the effective diffusion coefficient of oxygen within the flooded CL, n(=4) the number of exchanged electrons per oxygen molecule, and F(=96485 F·mol^{-1}) the Faraday constant. Boundary conditions at the membrane/CL and CL/GDL interfaces are, respectively

$$\text{x}=L_{CL} \qquad\qquad \mathrm{d}c/\mathrm{dx} = 0 \tag{3a}$$

$$\text{x}=0 \qquad\qquad c=c^0 \tag{3b}$$

where L_{CL} is the thickness of the catalyst layer, and c^0 is the oxygen concentration at the CL/GDL interface. The local current density (i) is described by Tafel kinetics:

$$i = c \, A_i \, i_0 \exp\left(\eta_{CL} \alpha nF/RT\right) / c^0 \tag{4}$$

where A_i (cm^2·cm^{-3}) is the internal CL electrochemical area, i_0 the exchange current density, η_{CL} the activation overpotential, α the transfer coefficient. From the solution of Eqs. (1)-(3), after substitution and integration in (4) over the whole CL, the expression for the total current density (i) is

$$i = n \, F \, D_{CL} \, c^0 \, a^{1/2} \tanh\left(a^{1/2} \, L_{CL}\right) \tag{5}$$

where

$$a = A_i \, i_0 \exp\left(\eta_{CL} \alpha nF/RT\right) / \left(n \, F \, D_{CL} \, c^0\right) \tag{6}$$

Eq. (5) describes current density (i) as a function of voltage loss due to activation and oxygen transport within the catalyst layer (η_{CL}). This expression is similar to that obtained for a microscopic model of a pore based on transmission line with equivalent circuit elements (de Levie 1967). The factor $1/a^{1/2}$ is the characteristic penetration depth of the electrochemical reaction within the CL, which is proportional to $(c^0 \cdot D_{CL})^{1/2}$ and inversely proportional to $(A_i \cdot i_0)^{1/2}$.

A second voltage loss in the cell is due to the internal resistance (R_i)

$$\eta_R = i \, R_i \tag{7}$$

Within the air breathing single cell the main contributions to this loss comes from electric contacts, specially between the grid collector and the cathode (R_{con}), and the ionic resistances of the membrane and the cathode catalyst layer ($R_{Mem}+R_{CL}$)

$$R_i = R_{CL} + R_{Mem} + R_{con} \tag{8}$$

Oxygen transport limitation within the GDL affects in two ways to voltage losses within the cell cathode: 1) the CL overpotential (η_{CL}) changes since oxygen reduction kinetics within the CL is affected through the parameter c^0 (Eqs. (5) and (6)); 2) mass transport loss within the GDL. Both

influences can be considered within the model. When oxygen transport within the cathode GDL is limiting, as it is the case at high enough current density, then the total current can be given by an expression for a linear diffusion layer (Bard and Faulkner 1980)

$$i = n\, F\, D_{GDL}\, (c^* - c^0)\, /\, L_{GDL} \tag{9}$$

Where c^* is the oxygen concentration at the GDL/air (Eq. (1)), and D_{GDL} the effective diffusion coefficient in the GDL. In order to consider the influence of oxygen mass transport limitation within the GDL on η_{CL}, c^0 from Eq. (9) can be substituted into Eqs. (5) and (6) to yield

$$i = n\, F\, D_{CL}\, c^*\, a^{*1/2}\, /(1/\tanh\, (a^{*1/2}L_{CL}) + D_{CL}L_{GDL}\, a^{*1/2}/D_{GDL}) \tag{10}$$

where a^* is now given by

$$a^* = A_i\, i_0 \exp\, (\eta_{CL}\alpha nF/RT)\, /\, (n\, F\, D_{CL}\, (c^* - i L_{GDL}/nFD_{GDL})) \tag{11}$$

Eqs. (10) and (11) form a system of equations with two unknowns (i and a^*) that can be solved by iterations procedure, taking from Eq. (6) the initial a^* value.

Since the experimental result is the polarization curve, which gives the current (i) as a function of cell voltage (V), the theoretical expression of interest for a cell dominated by the cathode voltage losses (the anode having minor contribution as is the case for AB-PEMFC operated with a constant hydrogen flux) is

$$V = E^0 - \eta_{CL} - i\, R_i - b\, \text{Log}\, (i_L/(i_L - i)) \tag{12}$$

Where η_{CL} and i are related by Eqs. (10) and (11). In Eq. (12) the third voltage loss term is due to mass transport within the GDL, as a function of the experimentally measured diffusion limiting current (i_L) (Bard and Faulkner 1980)

$$\eta_{GDL} = (RT/\alpha nF)\, \text{Ln}(i_L/(i_L - i)) \qquad = b\, \text{Log}(i_L/(i_L - i)) \tag{13}$$

Where $b(=2.303RT/\alpha nF)$ is the Tafel slope. The thermodynamic potential in Eq. (12) (E^0) can be calculated as a function of temperature (T) and partial pressures of hydrogen and oxygen (p_{H2}, p_{O2}) from (Neyerlin *et al.* 2006)

$$E^0 = 1.229 - 0.85 \cdot 10^{-3}\, (T\text{-}298.15) + 2.303\, RT\, \text{Log}\, (p_{H2}{}^2\, p_{O2}) \tag{14}$$

The model has been implemented in a Mathematica program to analyze polarization curves of AB-PEMFC prepared with cathodes differing in the CL thickness. Results are shown in the following section.

4. Results

4.1 Experimental results

Polarization and power density generation curves corresponding to three air breathing PEM single cells with variable cathode catalyst layer thickness (L_{CL}=8, 4 and 2.5 μm) are shown in Fig. 3. The cathodic catalyst layer were prepared by electrospray deposition of Pt/C+ionomer suspensions directly on the Nafion membrane, using commercial Pt/C catalysts with variable Pt/C ratio, and constant Pt loading (0.17 mg·cm^{-2}) and weight concentration of the ionomer (15% wt).
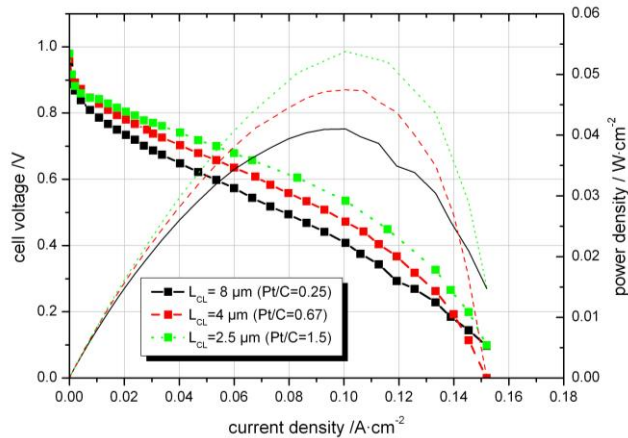
Fig. 3 Polarization curves and power density corresponding to three AB-PEMFC with variable cathodic catalyst layer thickness (L_{CL})
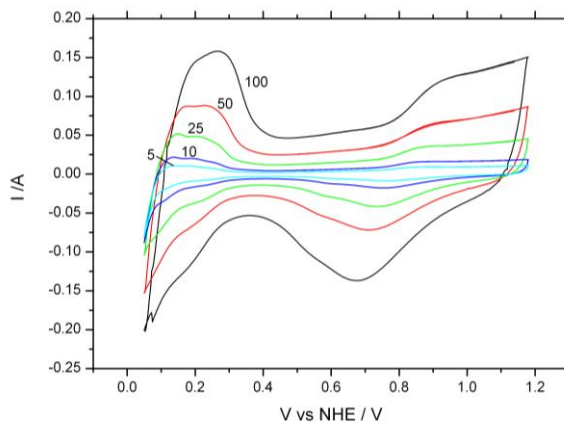

Fig. 4 Voltammetries at different scan rates (as indicated) for the determination of ECSA from H_{UPD} charge, corresponding to the an AB-PEMFC (L_{CL}=8μm) fed with static N_2 (1 bar) in the open cathode and flowing H_2 (20 cm^3·min^{-1}) in the anode

It is observed that decreasing L_{CL} gives rise to increase in performance and peak power density of the air-breathing cell. The values of the internal resistance of the cell, measured at 1kHz, are in the range of 0.5-0.6 Ohm·cm^2 (Table 1), which are a little higher compared with those measured on same cells but with a standard closed cathode flow field, typically in the range 0.2-0.3 Ohm·cm^2. The high R_i(1kHz) values of AB-PEMFC is attributed to flooded working conditions of the cathode as well as more resistive electric contact between the cathode and the current collector, both related with parameters R_{CL} and R_{con}, respectively (Eq. (8)).

The electrochemical active area (ECSA) of the three cathodes was measured with the underpotential hydrogen adsorption-desorption (H_{UPD}) method following the procedure described in ref. (Chaparro, Martín *et al.* 2009) which takes into account the finite diffusion rate of protons in the CL. According to this procedure, the real ECSA is taken from largest H_{UPD} charge measured
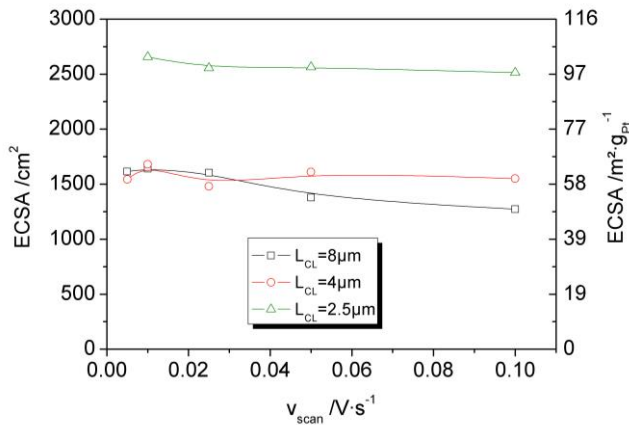
Fig. 5 Results of ECSA determination as a function of voltage scan rate

Table 1 Properties of the three CLs studied in this work

Catalyst wt% Pt	Pt/C	Nafion wt%	Nafion/C	L_{CL} µm	A_{HUPD} $m^2g_{Pt}^{-1}$	A_i cm^2cm^{-3}	R_i(1kHz) $Ohm \cdot cm^2$
20	0.25	15	0.21	8	62	131750	0.512
40	0.67	15	0.25	4	62	263500	0.617
60	1.5	15	0.28	2.5	100	629629	0.529

from voltammetries at different scan rates (Fig. 4). The voltammetries were obtained using the anode as reference and counter electrode, and saturating the ambient of the open cathode with N_2 gas by means of a cover with gas inlet and outlet.

Results of the electroactive area measurements for the three air breathing cathodes and as a function of voltage scan rate are shown in Fig. 5.

Area measurements show that the thickest CL 1(L_{CL}=8 µm) has larger dependence of the measured value with scan rate, than the other two thinner layers. Such dependence reflects more important proton diffusion limitation with thicker films (Chaparro, Martín *et al.* 2009). It is shown that the CL with 1 L_{CL}=2.5 µm has larger electrochemical area which may be attributed to different causes. On the one hand, properties of the CL vary with thickness, like Pt/C and Nafion/C ratios, that may favor Pt exposition to H^+ on thinner films. Also changes in the morphology and porosity of the electrosprayed layers have been observed with thickness that affect the ECSA. Finally the different carbon support used in the manufacture of the 60 wt% Pt/C catalyst may have improved the ECSA. A summary of properties of the three AB-PEMFCs is given in Table 1.

4.2 Analysis of polarization curves

The model described in Section 3 was applied to understand the effect observed of cathode catalyst thickness on the polarization curves of the AB-PEMFC (Fig. 3). For this analysis, starting value of parameters was taken from a literature survey. The exchange current density (i_0) for oxygen reduction on Pt surface in aqueous media takes values in the range 10^{-11}–10^{-9} A·cm^{-2} (Hoare 1967, Kinoshita 1992). For Pt nanoparticles supported on carbon, the measured value is

Table 2 Starting values used for polarization curves fitting

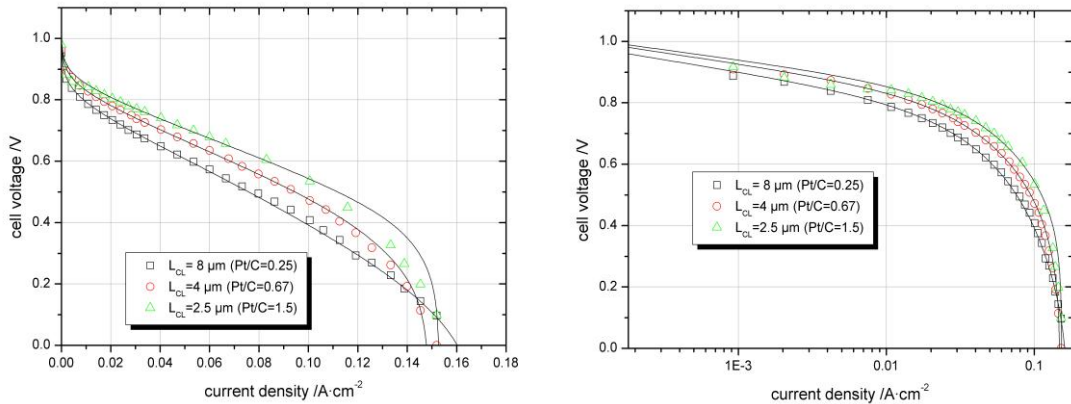| Parameter	Value	References
Exchange current density, i_0	$1.3 \cdot 10^{-9}$ A·cm^{-2}	Eikerling 2006, Jiang *et al.* 2012, Chaparro *et al.* 2009
Tafel slope, b	0.07 V	Jiang *et al.* 2012, Chaparro *et al.* 2009, Cruz-Manzo *et al.* 2010
Effective O_2 Diffusion coefficient in *CL*, D_{CL}	$2 \cdot 10^{-6}$ cm^2·s^{-1}	Liu *et al.* 2008
Effective O_2 Diffusion coefficient in *GDL*, D_{GDL}	$120 \cdot 10^{-4}$ cm^2·s^{-1}	Liu *et al.* 2008

Fig. 6 Linear and logarithmic representations of experimental (dot) and theory (line) curves corresponding to the fit of polarization curves in Fig. (3) to Eq. (12)

usually in the upper limit of this range (Eikerling 2006, Jiang *et al.* 2012). Our own values in previous works, obtained from polarization curves on electrospray deposited Pt/C cathodes at 80 ^{0}C, agree well with this value range (Chaparro *et al.* 2009, Chaparro *et al.* 2011, values in these references are referred to the geometric electrode area so conversion to real Pt area must be carried out). The Tafel slope (*b*), which characterizes the voltage loss due to reaction kinetics after tenfold increase of the reaction rate (current), takes usually a value around 0.07 V with little temperature influence, for oxygen reduction on Pt/C (Jiang *et al.* 2012, Cruz-Manzo *et al.* 2010, Parthasarathy *et al.* 1992). Oxygen diffusion within the catalyst layer is due to free molecular diffusion in larger pores and Knudsen diffusion in small pores. Both mechanisms can be described by a Fick's formula with an average diffusivity (Kulikovsky 2012). With air filled pores, the value of diffusivity at ambient temperature may be as large as $D_{eff}=10^{-3}$ cm^2·s^{-1}. However, when water accumulates within pores, oxygen diffusivity reduces significantly. A model by Liu and Eikerling (Liu *et al.* 2008) predicts diffusion coefficients values in dependence of water concentration, from $D_{eff}=2.1 \ 10^{-4}$ cm^2·s^{-1} when only primary pores are filled (r_p=1-10 nm), to $D_{eff}=2 \cdot 10^{-6}$ cm^2·s^{-1} when both primary and secondary pores (r_p=10-100 nm) are water filled. For the case of the air breathing cell the passive transport of water without assistance may render a completely flooded catalyst

Table 3 Parameters resulting from the fitting of polarization curves

Pt/C	L_{CL} μm	E^0 V	$10^9 \cdot i_0$ A·cm_{Pt}^{-2}	$\alpha \cdot n$	$b(=2.303RT/\alpha nF)$ V	$10^4 \cdot D_{CL}$ $cm^2 \cdot s^{-1}$	$10^4 \cdot D_{GDL}$ $cm^2 \cdot s^{-1}$	R_i (0Hz) Ohm·cm^2
0.25	8	1.219	0.8	0.76	0.078	2	168	2.6
0.67	4	1.219	0.7	0.84	0.070	3	145	2.3
1.50	2.5	1.219	0.3	0.92	0.064	5	149	2.0

layer so lowest value will be taken as initrial values. Oxygen diffusivity within the GDL is also strongly dependent on water content, from 10^{-5} to 10^{-3} $cm^2 \cdot s^{-1}$ according to the same study. A value of D_{GDL}=0.012 $cm^2 \cdot s^{-1}$ agrees with typical values from literature (Liu *et al.* 2008).

The fitting procedure was carried out by calculating the cell voltage (*V*) and current (*i*) taking the catalyst layer overpotential (η_{CL}) as independent variable, in the low and intermediate current range of the polarization curve, since at high current densities some model assumptions may not accomplish, like constant η_{CL} throughout the CL thickness, and conditions for water and oxygen transport in the GDL may be different. The values measured for A_i for the different electrodes where used for the fitting (Table 1).

Results of the fitting procedure are given in Fig. 6 and Table 3.

The results of the analysis reflect the influence of the cathodic catalyst layer thickness on the performance of the AB-PEMFC. The most important effect is encountered in the values of exchange current density (i_0), the Tafel slope (*b*) and the dc internal resistance (R_i). Similar effect of catalyst layer thickness on a standard single cell is observed by Lee *et al.* (2011). The results of the analysis are further commented in the following section.

5. Discussion

Values of the exchange current and Tafel slope, i_0 and *b* (Table 3), appear to show different effect of CL thickness on the oxygen reduction reaction within the cathode of the air breathing cells. Whereas a decrease in the exchange current density reflects a loss of kinetics performance, however it is accompanied by a decrease in Tafel slope that yields overall improvement of kinetics and cell response on thinner catalyst layers. The decrease of i_0 may be due to inference from parallel reactions in the cathode, like caused by carbon corrosion, that have larger influence in the low current regime where i_0 is determined. Carbon corrosion is accelerated by Pt, which acts as catalyst for this reaction, therefore it should have larger influence on i_0 determined on thinner catalyst layer. On the other hand, i_0 may also be influenced by the change in Nafion/C of the CLs (see Table 1), yielding different thickness of the ionomer film covering the catalyst, although Nafion ionomer film is not known to cause an important effect on the kinetics of the oxygen reduction.

On the other hand, the decrease of *b* with decreasing CL thickness reflects improvements of the oxygen reduction kinetics. The Tafel slope is related with the reaction mechanism in a complex way so a fundamental discussion in these terms is beyond the scope of this work. Clearly determining for thinner catalyst layers must be the larger proportion of platinum surface exposed to the electrolyte compared to carbon surface. Recent studies show that platinum and carbon surfaces have markedly different properties that affect the structure and distribution of the ionomer and catalyst within the film. Malek *et al.* (2011) conclude from a molecular dynamics study that
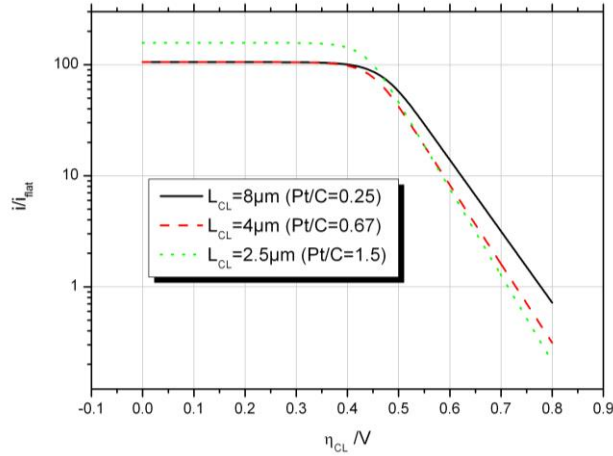
Fig. 7 Quotient of the current from porous and flat electrodes for parameters of the three cases studied in this work, and according to Eq. (16)

characteristics like particles agglomeration, ionomer film morphology, and arrangement of surface groups around catalyst particles, depend on the amount of platinum surface exposed. Results of capillary pressure show that platinum surface increases the hydrophilic character and water uptake by the ionomer, and, with it, the morphology and transport properties of the CL (Kusoglu *et al*. 2012). It is to be expected, therefore, that oxygen reduction conditions may be favored on thinner CL as a consequence of more hydrophilic character caused by larger platinum surface proportion.

It is also of interest to comment on the internal resistance values obtained for the different cells. A decrease in the dc internal resistance, R_i (0Hz) (Table 3), with thinner CL is expected simply because the cross sectional path for protons and electrons is shortened. However, it is to be noted that the high frequency internal resistance, i.e., that measured at 1kHz (Table 1), does not show the same trend, which may indicate that a fast charge conduction process is hindered by decreasing catalyst layer thickness. It is probable that the electronic conduction among catalyst particles (i.e., electrons must jump from one catalyst particle to another to arrive to the back contact of the electrode) becomes more resistive as a consequence of larger Nafion/C ratio, i.e., thicker ionomer film surrounding catalyst particles, and larger water content in the thinner and more hydrophilic catalyst layers. In fact, the increase in the internal resistance of single cells is observed if the ionomer concentration in the catalyst layer increases above a certain optimal value (Chaparro *et al*. 2009). A consequence of this analysis is that optimization of the ionomer concentration in the CL must be carried out as a function of L_{CL}.

The results show overall an improved CL behaviour when it is thinner. In principle, it could be concluded that thinner catalyst layer are desirable, and, in the limit, a flat catalyst layer would be the ideal for the cathode of the fuel cell. However, this is not the case as it can be inferred from model prediction. If the current density from a flat catalyst layer is given by

$$i_{flat} = c^0 \, i_0 \exp\left(\eta_{CL}\alpha nF/\text{RT}\right) / c^* \tag{15}$$

Then, the quotient of porous and flat catalyst layer, working both with same surface concentration (c^0) would be

$$i/i_{flat} = n\,F\,D_{CL}\,c^{*}\,a^{1/2}\,\tanh(a^{1/2}\,L_{CL})\,/\,(i_0\,\exp(\eta_{CL}\alpha nF/RT)) \qquad (16)$$

This quotient is plotted in Fig. 7 as a function of the overpotential, using parameters corresponding to the three catalyst layers studied in this work. It is shown that the flat catalyst layer would respond better than the porous catalyst layer only at large overpotentials ($\eta_{CL} > 0.7$V), which is a range difficult to attain in the real catalyst layer. The porous CL response would improve with respect to the flat electrode if it has good diffusional properties (D_{CL}), and large internal area (A_i), as well as with a high concentration of oxygen in the GDL.

6. Conclusions

The performance of AB-PEMFC has been studied as a function of CL thickness, by means of polarization curves. The analysis has been carried out on the basis of a theoretical model for a flooded cathode. The results show that catalyst layer thickness has influence both on oxygen reduction kinetics and charge transport, manifested by changes in the Tafel slope and the internal resistance of the cell. Thinner CL has improved oxygen reduction properties, which is attributed to more appropriate structural and hydrophilic conditions of CL.

Acknowledgements

References

Bard, A.J. and Faulkner, L.R. (1980), *Electrochemical Methods, Fundamentals and Applications*, John Wiley & Sons, New York.

Chang, H., Kim, J.R., Cho, J.H., Kim, H.K. and Choi, K.H. (2002), "Materials and processes for small fuel cells", *Solid State Ionics* **148**, 601-606.

Chaparro, A.M., Ferreira-Aparicio, P., Folgado, M.A., Martín, A.J. and Daza, L. (2011), "Catalyst layers for proton exchange membrane fuel cells prepared by electrospray deposition on nafion membrane", *J. Power Sources*, **196**, 4200-4208.

Chaparro, A.M., Gallardo, B., Folgado, M.A., Martín, A.J. and Daza, L. (2009), "PEMFC electrode preparation by electrospray: Optimization of catalyst load and ionomer content", *Catal. Today*, **178**, 237-241.

Chaparro, A.M., Martín, A.J., Folgado, M.A., Gallardo, B. and Daza, L. (2009), "Comparative analysis of the electroactive area of Pt/C PEMFC electrodes in liquid and solid polymer contact by underpotential hydrogen adsorption/desorption", *Int. J. Hydrogen Energy*, **34**, 4838-4846.

Cruz-Manzo, S., Rama, P. and Chen, R. (2010), "The low current electrochemical mechanisms of the fuel cell cathode catalyst layer through an impedance study", *J. Electrochem. Soc.*, **157**(3), B400-B408.

Cutlip, M.B. (1975), "An approximate model for mass transfer with reaction in porous gas diffusion electrodes", *Electrochim. Acta*, **20**, 767-773.

Eikerling, M. (2006), "Water management in cathode catalyst layers of PEM fuel cells. a structure-based model", *J. Electrochem. Soc.*, **153**(3), E58-E70.

Fernández-Moreno, J., Guelbenzu, G., Martín, A.J., Folgado, M.A., Ferreira-Aparicio, P. and Chaparro,

A.M. (2013), "A portable system powered with hydrogen and one single air-breathing PEM fuel cell", *App. Energy*, **109**, 60-66.

Giddey, S., Badwal, S.P.S., Ciacchi, F.T., Fini, D., Sexton, B.A., Glenn, F. and Leech, P.W. (2010), "Investigations on fabrication and lifetime performance of self – air breathing direct hydrogen micro fuel cells", *Int. J. Hydrogen Energy*, **35**, 2506-2516.

Heinzel, A., Hebling, C., Müller, M., Zedda, M. and Müller, C. (2002), "Fuel cells for low power applications", *J. Power Sources*, **105**, 250-255.

Hoare, J.P. (1967), *Advances in Electrochemistry and Electrochemical Engineering*, Vol. 6, Interscience, New York.

Jiang, J. and Kucernak, A. (2012), "Mass transport and kinetics of electrochemical oxygen reduction at nanostructured platinum electrode and solid polymer electrolyte membrane interface", *J. Sol. State Electrochem.*, **16**, 2571-2579.

Kinoshita, K. (1992), *Electrochemical Oxygen Technology*, John Wiley & Sons, New York.

Kulikovsky, A.A. (2012), "A physical model for catalyst layer impedance", *J. Electroanal. Chem.*, **669**, 28-34.

Kusoglu, A, Kwong, A., Clark, K.T., Gunterman, H.P. and Weber, A.Z. (2012), "Water uptake of fuel-cell catalyst layers", *J. Electrochem. Soc.*, **159**(9), F530-F535.

Lee, M., Uchida, M., Tryk, D.A., Uchida, H. and Watanabe, M. (2011), "The effectiveness of platinum/carbon electrocatalysts: Dependence on catalyst layer thickness and Pt alloy catalytic effects", *Electrochim. Acta*, **56**, 4783-4790.

de Levie, R. (1967), *Advances in Electrochemistry and Electrochemical Engineering*, Vol. 6, Interscience, New York.

Liu, L. and Eikerling, M. (2008), "Model of cathode catalyst layers for polymer electrolyte fuel cells: the role of porous structure and water accumulation", *Electrochim. Acta*, **53**, 4435-4446.

Malek, K., Mashio, T. and Eikerling, M. (2011), "Microstructure of catalyst layers in PEM fuel cells redefined: a computational approach", *Electrocatal.*, **2**, 141-157.

Meyers, J.P. and Maynard, H.L. (2002), "Design considerations for miniaturized PEM fuel cells", *J. Power Sources*, **109,** 76-88.

Neyerlin, k.C., Gu, W., Jorne, J. and Gasteiger, H.A. (2006), "Determination of Catalyst Unique Parameters for the Oxygen Reduction Reaction in a PEMFC", *J. Electrochem. Soc.*, **153**, A1955-A1963.

Parthasarathy, A., Srinivasan, S., Appleby, A.J. and Martin, C.R. (1992), "Pressure dependence of the oxygen reduction reaction at the platinum Microelectrode/Nafion interface: electrode kinetics and mass transport", *J. Electrochem. Soc.*, **139**(10), 2856-2862.

Stonehart, P. and Ross, P.N. (1976), "The use of porous electrodes to obtain kinetic rate constants for rapid reactions and adsorption isotherms of poisons", *Electrochim. Acta*, **21**, 441-445.

Vogel, W., Lundquist, J. and Bradford, A. (1972), "Reduction of oxygen on teflon-backed platinum black electrodes", *Electrochim. Acta*, **17**, 1735-1744.

Weiland, M., Wagner, S., Hahn, R. and Reichl, H. (2013), "Design and evaluation of a passive self-breathing micro fuel cell for autonomous portable applications", *Int. J. Hydrogen Energy*, **38,** 440-446.

CC